DOI: 10.1002/zaac.201300639

A Partially Fluorinated Three-fold Interpenetrated Stable Metal-Organic Framework with Selective CO_2 Uptake

Atanu Santra,[a] Myoung Soo Lah,*[b] and Parimal K. Bharadwaj*[a]

Dedicated to Professor C. N. R. Rao on the Occasion of His 80th Birthday

Keywords: Metal-organic frameworks; Fluorinated ligands; Selective CO_2 adsorption; Photoluminescence

Abstract. The hydrothermal reaction of $Zn(NO_3)_2{\cdot}H_2O$ and a linear 2,2′-bis-trifluoromethyl-biphenyl-4,4′-dicarboxylic acid (**H_2L**) ligand with $-CF_3$ groups at each phenyl moiety of the biphenyl rings leads to the formation of a three-fold interpenetrated metal-organic framework (MOF), $\{[Zn_{2.66}O_{0.66}(\mathbf{L})_2]{\cdot}2H_2O\}_n$ (**1**) at 180 °C. Single-crystal X-ray diffraction studies revealed that **1** is constructed from polynuclear clusters $[Zn_4O(COO)_6]$ as secondary building units (SBU). These SBU are connected through the $\mathbf{L}^{2-}$ to generate an overall three-dimensional structure with a 6-connected primitive cuboidal (α-Po) network. Thermogravimetric analyses and variable temperature powder X-ray diffraction measurements suggested that **1** is thermally stable. The porosity of **1** was estimated by N_2, CO_2, H_2, and CH_4 at different temperatures. The framework showed high selectivity of CO_2 uptake over N_2 and CH_4. Furthermore, solid-state photoluminescence studies were carried out for complex **1** upon excitation at 275 nm at room temperature.

Dedicated Issue

Introduction

The accumulation of carbon dioxide (CO_2), a greenhouse gas mainly responsible for global warming, has become one of the greatest environmental challenges worldwide.[1] Human activities, primarily increasing dependence on the combustion of fossil fuels (coal, petroleum, and natural gas) are largely increasing the concentration of CO_2 in the atmosphere.[2] As the major part of the flue gas is nitrogen (>70%) and the major impurity is CO_2 (10–15%), the separation of CO_2 from nitrogen is the key technical challenge. Another important separation involves removal of CO_2 from methane for quality upgradation of natural gas.[3] Adsorption method by MOFs is very promising for carbon capture and storage technology looking at energy required, cost, and properties of adsorbents.[4] However, the success of the approach is mainly dependent on developing suitable adsorbents with high adsorption capacity and selectivity of CO_2.

Emerging as a new class of porous materials for the last two decades, metal-organic frameworks (MOFs) have been receiving intensive research interest due to their tunable structures and porosities and a wide range of potential applications as functional materials.[5] Metal-organic frameworks (MOFs) built from metal ions and organic linkers that are low-density solids with extremely high surface area, are important in gas adsorption,[6] separation,[7] catalysis[8] and other applications.[9] Separation of CO_2 from other gases, viz. CO_2/N_2 (post combustion) and CO_2/CH_4 (natural gas purification), have high technological and industrial importance. It is within the abilities of chemists to systematically tune the pore size of MOFs via ligand design, to maximize the size-exclusive effects. Here, smaller molecules can go through the microporous channels, while larger substrates are blocked and immobilize functional sites such as open metal sites and functional groups, which direct their differential interactions with gas molecules. This has led microporous MOFs as very promising materials for practical gas adsorption and separation characteristics.[3,10] It has been found that some specific polar groups, for example $-CF_3$ or fluorine can be beneficial to selective CO_2 uptake due to the favorable electrostatic interactions with CO_2.[11] Besides, MOFs with fluoro-lined or fluoro-coated channels or cavities are expected to possess enhanced thermal and chemical stability, hydrophobicity and higher stability to oxidation and light.[12]

Herein, we have designed and synthesized a rigid linear ligand, 2,2′-bis-trifluoromethyl-biphenyl-4,4′-dicarboxylic acid (**H_2L**), which comprises two different functional groups, the terminal carboxylate groups will tend to form neutral MOFs, whereas the trifluoromethyl groups can act as secondary functional units in the pores (Scheme 1). Since Zn^{II} ions show a strong tendency to form $\{Zn_4O\}$ secondary building units (SBU) that provides strength to the overall structure, it has

* Prof. Dr. M. S. Lah
E-Mail: mslah@unist.ac.kr
* Prof. Dr. P. K. Bharadwaj
E-Mail: pkb@iitk.ac.in
[a] Department of Chemistry
Indian Institute of Technology
Kanpur, 208016, India
[b] Department of Chemistry
Ulsan National Institute of Science & Technology
Ulsan, 689–798, Korea
Supporting information for this article is available on the WWW under **http://dx.doi.org/10.1002/zaac.201300639** or from the author.

Zeitschrift für anorganische und allgemeine Chemie ZAAC Journal of Inorganic and General Chemistry

been taken in the presented study.[13] During the course of the present studies, the zinc cluster based three-fold interpenetrated porous framework $\{[Zn_{2.66}O_{0.66}(\mathbf{L})_2]\cdot 2H_2O\}_n$ (**1**) was reported. It shows high thermal as well as moisture stability and can be easily synthesized via hydrothermal technique. The framework exhibits permanent porosity, high selectivity, and storage capacity for CO_2 over nitrogen and methane at low pressure. Solid-state photoluminescence studies for complex **1** were also investigated upon excitation at 275 nm at room temperature.

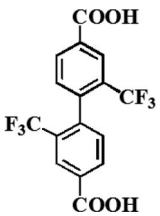

Scheme 1. 2,2′-Bis-trifluoromethyl-biphenyl-4,4′-dicarboxylic acid ($\mathbf{H_2L}$).

Results and Discussion

Compound $\{[Zn_{2.66}O_{0.66}(\mathbf{L})_2]\cdot 2H_2O\}_n$ (**1**) was synthesized by hydrothermal reaction using $Zn(NO_3)_2\cdot 6H_2O$ and $\mathbf{H_2L}$ as starting materials at 180 °C for 72 h. Once isolated, **1** is found to be air-stable and insoluble in common organic solvents as well as in water. In the IR spectrum of **1**, broad bands around 3416 cm^{-1} suggest the presence of lattice water molecules, whereas the sharp peak at 1614 cm^{-1} is attributable to C=O stretching vibrations of metal coordinated carboxylate groups (Figure S1, Supporting Information).[14] Single crystal X-ray analysis reveals that the structure can be converged successfully in the trigonal space group $R\bar{3}$.

The asymmetric unit consists of four crystallographically independent Zn^{II} ions (two with full occupancy and other two with one-third occupancy), two $\mathbf{L}^{2-}$ and two μ_4-O^{2-} ions (with one-third occupancy) (Figure 1). All the Zn^{II} ions are tetra-coordinated with ligation from three carboxylate oxygen atoms [Zn–O = 1.92(5)–2.12(7) Å] from three $\mathbf{L}^{2-}$ ligands and one oxygen atom [Zn–O = 1.82(5)–1.95(3) Å] from the bridging μ_4-O^{2-} ions. The framework contains polynuclear clusters as its secondary building units (SBUs): one distinct $[Zn_4O(COO)_6]$ and a $[Zn_4O(COO)_6]$ that is positionally disordered and looks like a $[Zn_8O_2(COO)_{12}]$ (Figure 2).

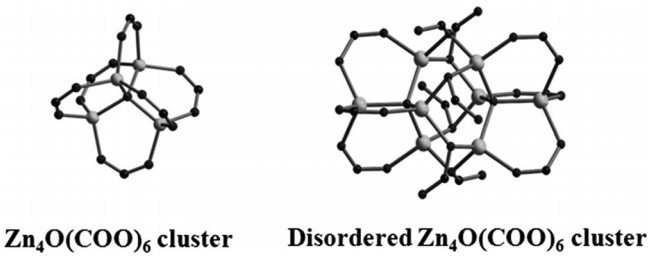

Figure 2. Perspective view of the SBUs present in **1**.

Each $[Zn_4O(COO)_6]$ SBU is connected to the six neighboring $[Zn_4O(COO)_6]$ SBUs by six $\mathbf{L}^{2-}$ (Figure 3) to generate a three-fold interpenetrated cubane-like framework (Figure 4). Though the interpenetration reinforced the framework stability,

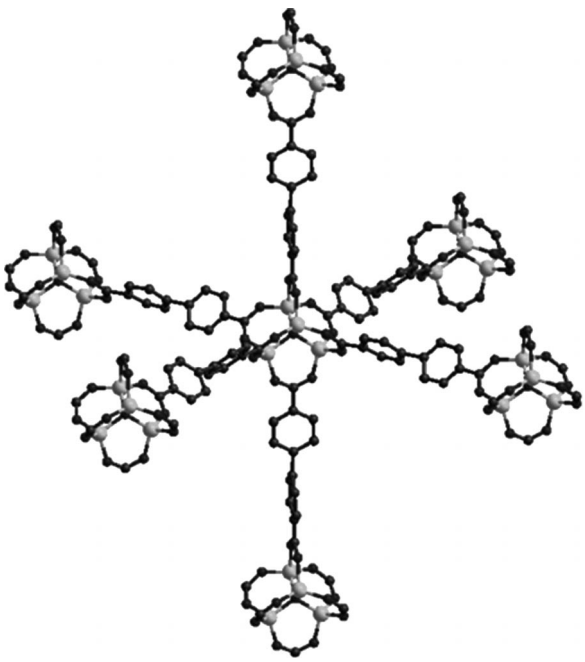

Figure 3. 3D view of the network $[Zn_4O(COO)_6]$ SBUs connected via ligand (hydrogen and $-CF_3$ are omitted for clarity).

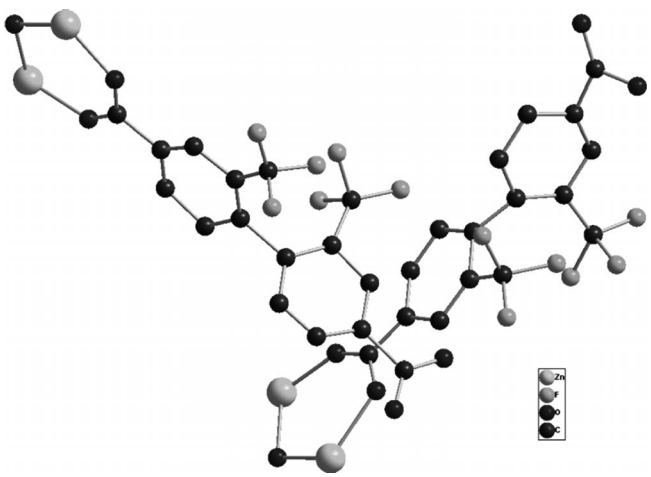

Figure 1. Perspective view of the asymmetric unit of **1** (hydrogen atoms are omitted for clarity).

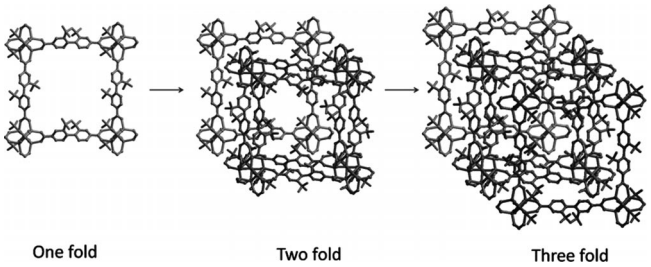

Figure 4. Consecutive representation of (a) one fold, (b) two fold and (c) three-fold interpenetrated framework.

but it reduces the pore dimension.[15] The framework contains fluorine decorated wave like unsymmetrical pore (Figure 5).

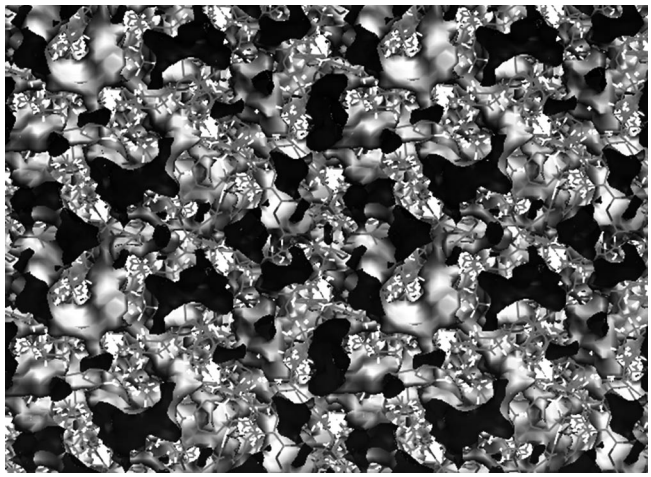

Figure 5. Perspective view of wave like unsymmetrical pores in **1**.

Solvent accessible volume calculated from the crystal structure using the PLATON routine[16] is 23.5 % of the total crystal volume. Topological simplification with Topos software[17] shows that the compound belongs to three-fold interpenetrated 6-connected **pcu** network (α-Po).

Stability of the Framework

Thermogravimetric analyses (TGA) and variable temperature powder X-ray diffraction (VTPXRD) measurements were carried out to examine the thermal stability of the framework. The TGA curve (Figure S2, Supporting Information) reveals a weight loss of 3.8 % up to 95 °C corresponding to loss of H_2O molecules present in the lattice (calculated 3.7 %). No further weight loss is observed till 450 °C and complete decomposition is achieved beyond this temperature.

Thermal stability and phase purity of **1** was also confirmed by variable temperature PXRD (Figure 6). It clearly reveals the overall framework structure to be intact at least up to 350 °C.

The stability of compound in presence of water vapor was studied. The desolvated sample was taken in glass vial and kept in slightly bigger screw cap bottle containing water. The PXRD of the sample was recorded after different time intervals. The framework stability was confirmed from PXRD pattern (Figure 7). However, most MOFs, in particular zinc-based MOFs, are moisture-sensitive as the weak metal-oxygen coordination allows for attack by water molecules, resulting in the phase transformation and decomposition of the framework.[18] Here, the water stability of this framework might be due to the presence of hydrophobic functional groups like $–CF_3$ in the framework, which makes it water resistant.[19]

Adsorption Studies

The 3D framework with high thermal stability and structural rigidity that maintains the overall structure upon solvent removal as revealed by VTPXRD makes compound **1** a potential candidate for gas adsorption. To evaluate porosity of the activated **1**, gas adsorption experiments were carried out with N_2, H_2, CO_2, and CH_4 under different experimental conditions. The nitrogen adsorption shows a typical type-I behavior (Figure 8). The BET surface area is estimated to be 780 $m^2 \cdot g^{-1}$ and

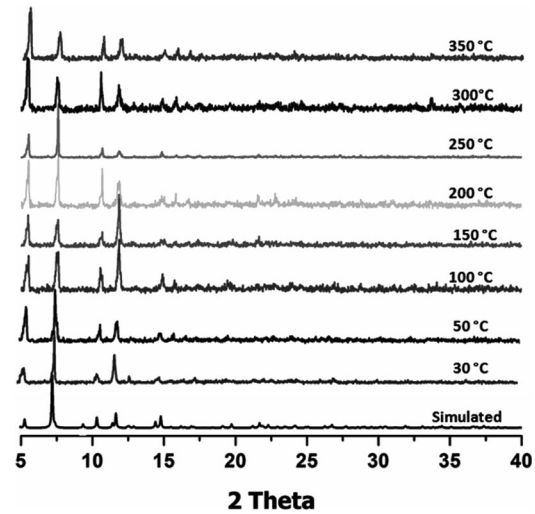

Figure 6. Variable temperature PXRD pattern of complex **1**.

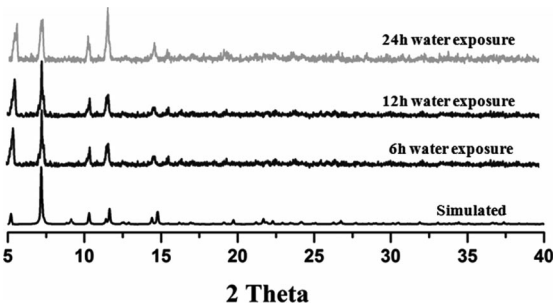

Figure 7. PXRD patterns for complex **1** after exposure to water vapor for 6 h, 12 h, and 24 h.

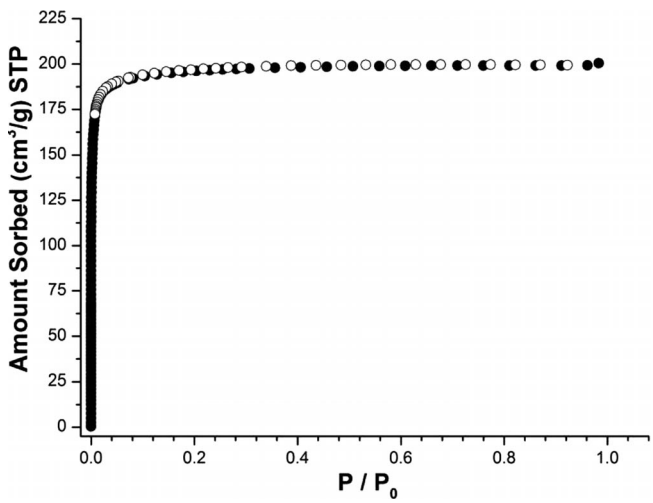

Figure 8. Nitrogen physisorption isotherm of activated **1** at 77 K (adsorption/desorption ●/○).

Zeitschrift für anorganische und allgemeine Chemie ZAAC Journal of Inorganic and General Chemistry

the Langmuir surface area as 867 $m^2 \cdot g^{-1}$ for all pressure ranges. The measured pore volume of **1** from the N_2 sorption (at P/P_0 = 0.983) is found to be 0.310 $cm^3 \cdot g^{-1}$.

The adsorption isotherms of CO_2 and CH_4 at 196 K were carried out. Interestingly, the CO_2 physisorption isotherms at 196 K (Figure 9) exhibit deviation from a typical type-I behavior. Initially it shows a steep rise at very low pressure region (P/P_0 = 0.2), and then attains saturation with the adsorbed CO_2 amount of 156.86 $cm^3 \cdot g^{-1}$ (6.998 $mmol \cdot g^{-1}$). A hysteresis between the adsorption and desorption is observed, which might be due to the trapping effect of the gas in the fluorine decorated wave like unsymmetrical pore. Such behavior is not unprecedented.[6b] The CH_4 adsorption amount at P/P_o = 0.992 is 60.01 $cm^3 \cdot g^{-1}$(2.677 $mmol \cdot g^{-1}$).

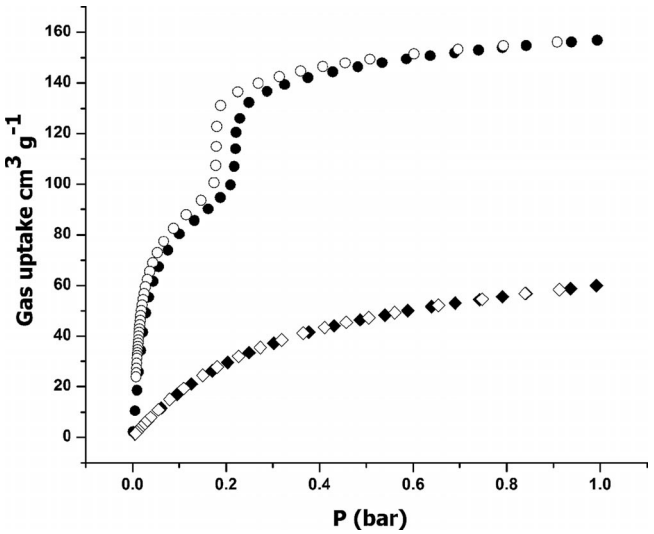

Figure 9. Selective adsorption of CO_2 (●/○) over CH_4 (■/□) of activated **1** at 196 K (filled balls: adsorption, empty balls: desorption).

To determine the adsorption selectivity and capacity of **1** the adsorption/desorption isotherms of CO_2 and N_2 were measured at 273 K (Figure 10). The CO_2 uptake of **1** at 273 K and P/P_0 = 0.9936 is 32.281$cm^3 \cdot g^{-1}$(1.440 $mmol \cdot g^{-1}$). But at the same experimental condition, it can hardly adsorb N_2 (0.294 $cm^3 \cdot g^{-1}$). Although the CO_2 uptake ability of **1** is at moderate level compared to some currently reported MOFs, it exhibits high CO_2 adsorption selectivity over N_2 at ambient condition. The uptakes of CO_2 and N_2 at 273 K and P/P_0 = 0.9936 were used to estimate the adsorption selectivity for CO_2 over N_2.[20] From these data, the calculated CO_2/N_2 adsorption selectivity is 109.7 at 273 K. MOFs with such high CO_2/N_2 adsorption selectivity at ambient conditions are rarely known.[21] The isosteric heat of CO_2 adsorption calculated using the virial method is 22.9 $kJ \cdot mol^{-1}$ at low coverage (Figure 11).

The high selectivity of CO_2, having higher polarizability over N_2 may be induced by the strong polar environment in the pore. In view of the structural feature of **1**, such gas-adsorption selectivity might be associated with the presence of the polar $–CF_3$ groups, giving rise to an electric field to induce a dipole in CO_2 and an interaction between CO_2 and $–CF_3$.[11]

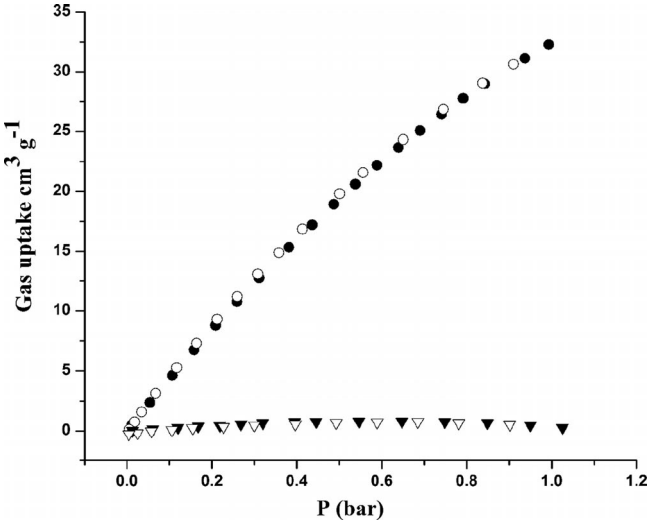

Figure 10. Selective adsorption of CO_2 (●/○) over N_2 (▲/Δ) of activated **1** at 273 K (filled balls: adsorption, empty balls: desorption).

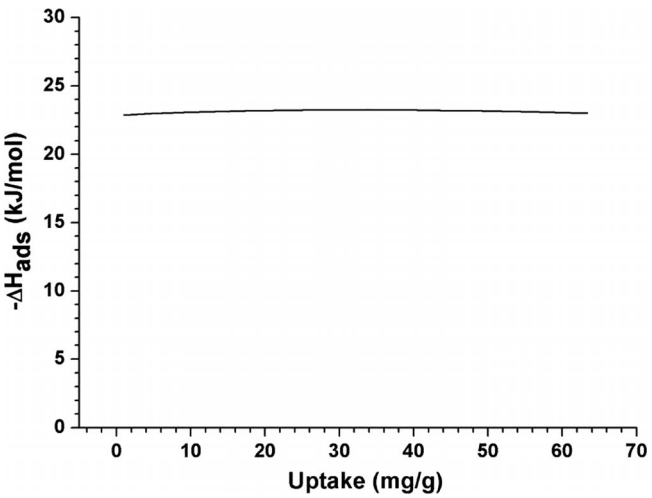

Figure 11. Isosteric heat of adsorption in dependence of the CO_2 uptake.

The interpenetration and $–CF_3$ functionalization make the framework suitable for H_2 adsorption.[15,11] The H_2 sorption of **1** was studied at 77 K and up to 1 bar it exhibits a typical reversible type-I isotherm with a capacity of 113.88 $cm^3 \cdot g^{-1}$(1.02 wt%) (Figure 12). Though the H_2 storage capacity of **1** is moderate, it is comparable to many reported MOFs.[6a]

Photoluminescence Properties

Coordination polymers with central d^{10} metal atoms and conjugated carboxylate-based organic linkers are considered as a promising option for photoactive materials with potential applications in photochemistry, chemical sensors, as well as in electroluminescent displays.[22] In this regard, the solid state photoluminescence properties of the complex **1** and **H_2L** ligand have been explored at room temperature and are shown

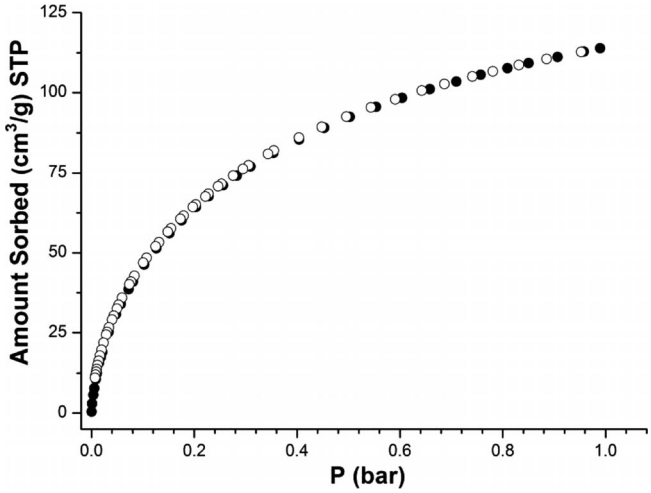

Figure 12. Hydrogen physisorption isotherms of activated **1** at 77 K (adsorption/desorption ●/○).

collectively in Figure 13. It is observed that the metal-free **H_2L** exhibits an emission band maximum at 421 nm with excitation at 275 nm. These emission bands of free ligand can probably be assigned to the π→π* transition.[23,9a] Irradiation of crystalline complex **1** with ultraviolet light (λ_{ex} = 275 nm) at room temperature results in broad unsymmetrical emissions. Since the profile of the emission band is quite similar to that of the metal-free ligand, the emission of **1** could be attributed to the intra-ligand (π–π*) emission.

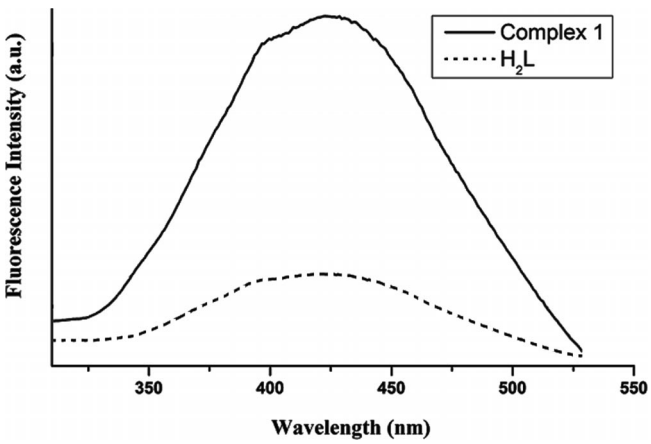

Figure 13. Solid state luminescent spectra at room temperature.

Conclusions

By using the ligand 2,2′-bis-trifluoromethyl-biphenyl-4,4′-dicarboxylic acid (**H_2L**), a three-fold interpenetrated metal organic framework could be synthesized and characterized. Solid-state emissions of the complex were explored at room temperature. The complex exhibits a very high selectivity and storage capacity for CO_2 over N_2 and CH_4. High thermal stability, as well as selective capture of CO_2, makes the compound a promising candidate for industrial gas separation and environmental process. Further investigations on related partially fluorinated MOFs are in progress to better understand the sorption properties of these frameworks.

Experimental Section

Materials: The metal salt and other reagent grade chemicals were procured from Sigma-Aldrich and used as received. All the solvents were from S. D. Fine Chemicals, India. These solvents were purified following standard methods prior to use.

Physical Measurements: Infrared (IR) spectra (KBr disk, 400–4000 cm^{-1}) were recorded with a Perkin-Elmer Model 1320 spectrometer. Thermogravimetric analyses (TGA) (5 °C·min^{-1} heating rate in a nitrogen atmosphere) were performed with a Mettler Toledo Star System. Microanalyses for the compounds were carried out with a CE-440 elemental analyzer (Exeter Analytical Inc.). Powder X-ray diffraction (PXRD) studies were carried out with a Bruker D8 Advanced powder diffractometer with Cu-K_α radiation. Solid-state photoexcitation and emission spectra were recorded with a double UV/Vis/NIR spectrophotometer (Varian Model Cary 5000) and Jobin Yvon Horiba Fluorolog-3 spectrofluorimeter at room temperature.

Synthesis of the Ligand H_2L: The ligand 2,2′-bis-trifluoromethyl-biphenyl-4,4′-dicarboxylic acid (**H_2L**) was synthesized following a previously reported procedure.[24]

Synthesis of $\{[Zn_{2.66}O_{0.66}(L)_2]\cdot 2H_2O\}_n$ (1): A mixture containing **H_2L** (0.03 g, 0.10 mmol), $ZnNO_3\cdot 6H_2O$ (0.031 g, 0.10 mmol), and H_2O (4 mL) was placed in a Teflon-lined autoclave, heated under autogenous pressure to 180 °C for 72 h, and allowed to cool to room temperature at the rate of 1 °C per min. Rectangular-shaped colorless crystals of **1** were collected and washed with H_2O followed by EtOH and finally dried in air. Yield ca. 47%. $C_{96}H_{45}F_{36}O_{32}Zn_8$: calcd. C 39.65; H 1.54%; found: C 39.73; H 1.61%. **IR** (KBr): $\tilde{\nu}$ = 3416 (broad), 3085 (broad), 1614 (s), 1548 (m), 1435 (s) cm^{-1}.

X-ray Structural Studies: Single crystal X-ray data on **1** was collected at 100 K with a Bruker SMART APEX CCD diffractometer using graphite-monochromated Mo-K_α radiation (λ = 0.71073 Å). The linear absorption coefficients, scattering factors for the atoms, and the anomalous dispersion corrections were taken from International Tables for X-ray Crystallography. The data integration and reduction were processed with SAINT[25] software. An empirical absorption correction was applied to the collected reflections with SADABS[26] using XPREP.[27] The structure was solved by the direct method using SIR-97[28] and was refined on F^2 by full-matrix least-squares technique using the SHELXL-97[29] program package. The non-hydrogen atoms were refined anisotropically. Hydrogen atoms were placed in calculated positions using idealized geometries (riding model) and assigned fixed isotropic displacement parameters using SHELXL default. The trifluoromethyl groups, biphenyl ring as well as a $Zn_4O(COO)_6$ cluster were disordered. For this, several DFIX commands were used to fix the bond lengths. To give an account of disordered electron densities associated with solvent molecules in **1**, the "squeeze" protocol in the PLATON package[16] was applied. The contribution of all the solvent atoms has been incorporated in both the empirical formula and formula weight of the complex. The crystal and refinement data are collected in Table 1, whereas bond lengths and bond angles are collected in Table S1 (Supporting Information).

Zeitschrift für anorganische und allgemeine Chemie ZAAC Journal of Inorganic and General Chemistry

Table 1. Crystal and structure refinement data for **1**.

	1
Formula	$C_{96}H_{45}F_{36}O_{32}Zn_8$
Formula weight	2905.19
Temperature /K	100
Radiation	Mo-K_α
Wavelength /Å	0.71073
Crystal system	trigonal
Space group	$R\bar{3}$
a /Å	24.577(5)
b (Å	24.577(5)
c /Å	28.997(4)
α /°	90.000
β /°	90.000
γ /°	120.000
V /Å^3	15169(8)
Z	6
ρ_{calc} g·cm^{-3}	1.845
μ /mm^{-1}	2.006
F(000)	8286
Refl. collected	25094
R_{int}	0.1062
Independent refl.	3484
Refinement method	Full-matrix least- squares on F^2
GOF	1.255
Final R indices [$I>2\sigma$ (I)]	R_1 = 0.1457 wR_2 = 0.3690
R indices (all data)	R_1 = 0.1848 wR_2 = 0.3894

Crystallographic data (excluding structure factors) for the structure in this paper have been deposited with the Cambridge Crystallographic Data Centre, CCDC, 12 Union Road, Cambridge CB21EZ, UK. Copies of the data can be obtained free of charge on quoting the depository number CCDC-974633 (Fax: +44-1223-336-033; E-Mail: deposit@ccdc.cam.ac.uk, http://www.ccdc.cam.ac.uk).

Physisorption Measurements: All gas sorption isotherms were measured with a BELSORP-max (BEL Japan, Inc.) with a standard volumetric technique up to saturated pressure. Before the sorption study, the samples were soaked in dichloromethane for overnight, and activated for 12 h in vacuo at 80 °C. The adsorption data in the pressure range for 0.002–0.081 P/P_o were fitted to the Brunauer-Emmett-Teller (BET) equation to determine the BET surface areas. The N_2 and H_2 sorption isotherms were monitored at 77 K. The CO_2 sorption isotherms were measured at both 273 and 196 K; CH_4 sorption isotherms were measured at 196 K. High purity gases were used for the adsorption measurements (nitrogen: 99.999%, hydrogen: 99.999%, CO_2: 99.99%, methane: 99.99%).

Supporting Information (see footnote on the first page of this article): Table for selected bonds and distances for **1** and complete data for IR and TGA analysis.

Acknowledgements

We gratefully acknowledge the financial support received from the Department of Science and Technology, New Delhi, India (to PKB) and SRF from the CSIR to A.S. M.S.L. acknowledges financial support from the NRF of Korea (2012R1A2A2A01003077).

References

[1] a) D. M. D'Allessandro, B. Smit, J. R. Long, *Angew. Chem. Int. Ed.* **2010**, *49*, 6058–6082; b) Y.-S. Bae, R. Q. Snurr, *Angew. Chem. Int. Ed.* **2011**, *50*, 11586–11596; c) H. S. Choi, M. P. Suh, *Angew. Chem. Int. Ed.* **2009**, *48*, 6865–6870.

[2] a) IPCC, 2007: *Summary for Policymakers*, in *Climate Change 2007: The Physical Science Basis*, Cambridge University Press, Cambridge, UK, **2007**; b) M. Z. Jacobson, *Energy Environ. Sci.* **2009**, *2*, 148–173.

[3] K. Sumida, D. L. Rogow, J. A. Mason, T. M. McDonald, E. D. Bloch, Z. R. Herm, T.-H. Bae, J. R. Long, *Chem. Rev.* **2012**, *112*, 724–781.

[4] a) M. O'Keefe, M. A. Peskov, S. J. Ramsden, O. M. Yaghi, *Acc. Chem. Res.* **2008**, *41*, 1782–1789; b) S. Cavenati, C. A. Grande, A. E. Rodrigues, *J. Chem. Eng. Data* **2004**, *49*, 1095–1099; c) R. Vaidhyanathan, S. S. Iremonger, G. K. H. Shimizu, P. G. Boyd, S. Alavi, T. K. Woo, *Science* **2010**, *330*, 650–653.

[5] a) G. Férey, *Chem. Soc. Rev.* **2008**, *37*, 191–214; b) J.-R. Li, R. J. Kuppler, H.-C. Zhou, *Chem. Soc. Rev.* **2009**, *38*, 1477–1504; c) A. Phan, C. Doonan, F. J. Uribe-Romo, C. B. Knobler, M. O'Keeffe, O. M. Yaghi, *Acc. Chem. Res.* **2009**, *42*, 58–67; d) S. Kitagawa, R. Kitaura, S. Noro, *Angew. Chem. Int. Ed.* **2004**, *43*, 2334–2375.

[6] a) M. P. Suh, H. J. Park, T. K. Prasad, D.-W. Lim, *Chem. Rev.* **2012**, *112*, 782–835; b) M. K. Sharma, I. Senkovska, S. Kaskel, P. K. Bharadwaj, *Inorg. Chem.* **2011**, *50*, 539–544; c) S. S. Nagarkar, A. K. Chaudhari, S. K. Ghosh, *Inorg. Chem.* **2012**, *51*, 572–576; d) Y.-Q. Lan, H.-L. Jiang, S.-L. Li, Q. Xu, *Adv. Mater.* **2011**, *23*, 1015–1520.

[7] a) H.-L. Jiang, Y. Tatsu, Z.-H. Lu, Q. Xu, *J. Am. Chem. Soc.* **2010**, *132*, 5586–5587; b) M. C. Das, P. K. Bharadwaj, *J. Am. Chem. Soc.* **2009**, *131*, 10942–10949; c) L. Duan, Z.-H. Wu, J.-P. Ma, X.-W. Wu, Y.-B. Dong, *Inorg. Chem.* **2010**, *49*, 11164–11173; d) J.-R. Li, J. Sculley, H.-C. Zhou, *Chem. Rev.* **2012**, *112*, 869–932.

[8] a) L. Ma, J. M. Falkowski, C. Abney, W. Lin, *Nat. Chem.* **2010**, *2*, 838–846; b) J. M. Roberts, B. M. Fini, A. A. Sarjeant, O. K. Farha, J. T. Hupp, K. A. Scheidt, *J. Am. Chem. Soc.* **2012**, *134*, 3334–3337; c) R. K. Das, A. Aijaz, M. K. Sharma, P. Lama, P. K. Bharadwaj, *Chem. Eur. J.* **2012**, *18*, 6866–6872.

[9] a) Y. Cui, Y. Yue, G. Qian, B. Chen, *Chem. Rev.* **2012**, *112*, 1126–1162; b) J. An, S. J. Geib, N. L. Rosi, *J. Am. Chem. Soc.* **2009**, *131*, 8376–8377; c) P. Lama, A. Aijaz, E. C. Sañudo, P. K. Bharadwaj, *Cryst. Growth Des.* **2010**, *10*, 283–290; d) M. Ahmad, M. K. Sharma, R. Das, P. Poddar, P. K. Bharadwaj, *Cryst. Growth Des.* **2012**, *12*, 1571–1578.

[10] a) T. K. Kim, M. P. Suh, *Chem. Commun.* **2011**, *47*, 4258–4260; b) J. Zhang, H. Wu, T. J. Emge, J. Li, *Chem. Commun.* **2010**, *46*, 9152–9154.

[11] a) C. Yang, X. P. Wang, M. A. Omary, *J. Am. Chem. Soc.* **2007**, *129*, 15454–15455; b) Z. Hulvey, E. H. L. Falcao, J. Eckert, A. K. Cheetham, *J. Mater. Chem.* **2009**, *19*, 4307–4309; c) P. Kanoo, S. K. Reddy, G. Kumari, R. Haldar, C. Narayana, S. Balasubramanian, T. K. Maji, *Chem. Commun.* **2012**, *48*, 8487–8489; d) A. Santra, I. Senkovska, S. Kaskel, P. K. Bharadwaj, *Inorg. Chem.* **2013**, *52*, 7358–7366.

[12] a) C. Yang, X. P. Wang, M. A. Omary, *Angew. Chem. Int. Ed.* **2009**, *48*, 2500–2505; b) *Handbook of Fluorous Chemistry* (Eds.: J. A. Gladysz, D. P. Curran, I. T. Horváth), Wiley-VCH, Weinheim, Germany, **2004**.

[13] M. Eddaoudi, J. Kim, N. Rosi, D. Vodak, J. Wachter, M. O'Keeffe, O. M. Yaghi, *Science* **2002**, *295*, 469–472.

[14] a) R. Singh, M. Ahmad, P. K. Bharadwaj, *Cryst. Growth Des.* **2012**, *12*, 5025–5034; b) J. Sahu, M. Ahmad, P. K. Bharadwaj, *Cryst. Growth Des.* **2013**, *13*, 2618–2627.

[15] a) H. Kim, S. Das, M. G. Kim, D. N. Dybtsev, Y. Kim, K. Kim, *Inorg. Chem.* **2011**, *50*, 3691–3696; b) B. Chen, S. Ma, E. J. Hurtado, E. B. Lobkovsky, H.-C. Zhou, *Inorg. Chem.* **2011**, *50*, 8490–8492.

[16] A. L. Spek, *PLATON*, The University of Utrecht, The Netherlands, **1999**.

[17] The network topology was evaluated by the program *TOPOS-4.0*, see: http://www.topos.ssu.samara.ru; a) V. A. Blatov, *IUCr Compcomm. Newsletter* **2006**, *7*, 4; b) V. A. Blatov, M. O'Keeffe,

Dedicated Issue

D. M. Proserpio, *CrystEngComm* **2010**, *12*, 44–48; c) V. A. Blatov, A. P. Shevchenko, V. N. Serezhkin, *J. Appl. Crystallogr.* **2000**, *33*, 1193.
[18] a) M. Dinca, J. R. Long, *J. Am. Chem. Soc.* **2007**, *129*, 11172–11176; b) K. Schrock, F. Schroder, M. Heyden, R. A. Fischer, M. Havenith, *Phys. Chem. Chem. Phys.* **2008**, *10*, 4732–4739; c) K. S. Park, Z. Ni, A. P. Cote, J. Y. Choi, R. Huang, F. J. Uribe-Romo, H. K. Chae, M. O'Keeffe, O. M. Yaghi, *Proc. Natl. Acad. Sci. USA* **2006**, *103*, 10186–10191.
[19] a) J. B. Decoste, G. W. Peterson, M. W. Smith, C. A. Stone, C. R. Willis, *J. Am. Chem. Soc.* **2012**, *134*, 1486–1489; b) J. Yang, A. Grzech, F. M. Mulderb, T. J. Dingemans, *Chem. Commun.* **2011**, *47*, 5244–5246; c) T.-H. Chen, I. Popov, O. Zenasni, O. Daugulis, O. Š. Miljanic, *Chem. Commun.* **2013**, *49*, 6846–6848.
[20] Y. Jin, B. A. Voss, R. D. Noble, W. Zhang, *Angew. Chem. Int. Ed.* **2010**, *49*, 6348–6351.
[21] K. Sumida, S. Horike, S. S. Kaye, Z. R. Herm, W. L. Queen, C. M. Brown, F. Grandjean, G. J. Long, A. Dailly, J. R. Long, *Chem. Sci.* **2010**, *1*, 184–191.
[22] a) C. W. Tang, S. A. Vanslyke, *Appl. Phys. Lett.* **1987**, *51*, 913–915; b) M. D. Allendorf, C. A. Bauer, R. K. Bhakta, R. J. T. Houk, *Chem. Soc. Rev.* **2009**, *38*, 1330–1352.
[23] a) X. J. Zhang, L. P. Jin, S. Gao, *Inorg. Chem.* **2004**, *43*, 1600–1602; b) M. Ahmad, P. K. Bharadwaj, *Polyhedron* **2013**, *32*, 1145–1152.
[24] J.-C. Chen, C.-J. Hing, Y.-C. Liu, *Synth. Met.* **2010**, *160*, 1953–1961.
[25] *SAINT+*, 6.02 ed.; Bruker AXS, Madison, WI, **1999**.
[26] G. M. Sheldrick, *SADABS*, Empirical Absorption Correction Program, University of Göttingen, Germany, **1997**.
[27] *XPREP*, 5.1 ed. Siemens Industrial Automation Inc., Madison, WI, USA, **1995**.
[28] G. M. Sheldrick, *SHELXTL*, Version 5.1, Bruker AXS, Madison, WI, USA, **1997**.
[29] G. M. Sheldrick, *SHELXL-97*, Program for Crystal Structure Refinement, University of Göttingen, Göttingen, Germany, **1997**.

Received: December 11, 2013
Published Online: January 12, 2014

